MAE 598 Design Optimization Project 2:

ANSYS Design of Experiments (DOE) and Optimization of Brake Disc

Jessica Westerham

Professor Yi Ren

Arizona State University

November 17, 2021

Objective

This project simulates the Design of Experiment (DOE) and the iterative design optimization of a brake disc. The simulations were conducted based on the tutorial from ANSYS DOE and Design Optimization Tutorial by Y. Ren and A. Vipradas. The model was downloaded from the brake.agdb file provided by Design Optimization of Brake Disc Geometry (2016) by A. Durgude, A. Vipradas, S. Kishore, and S. Nimse. An image of the brake disc with the two brake pads is shown in Figure 1.

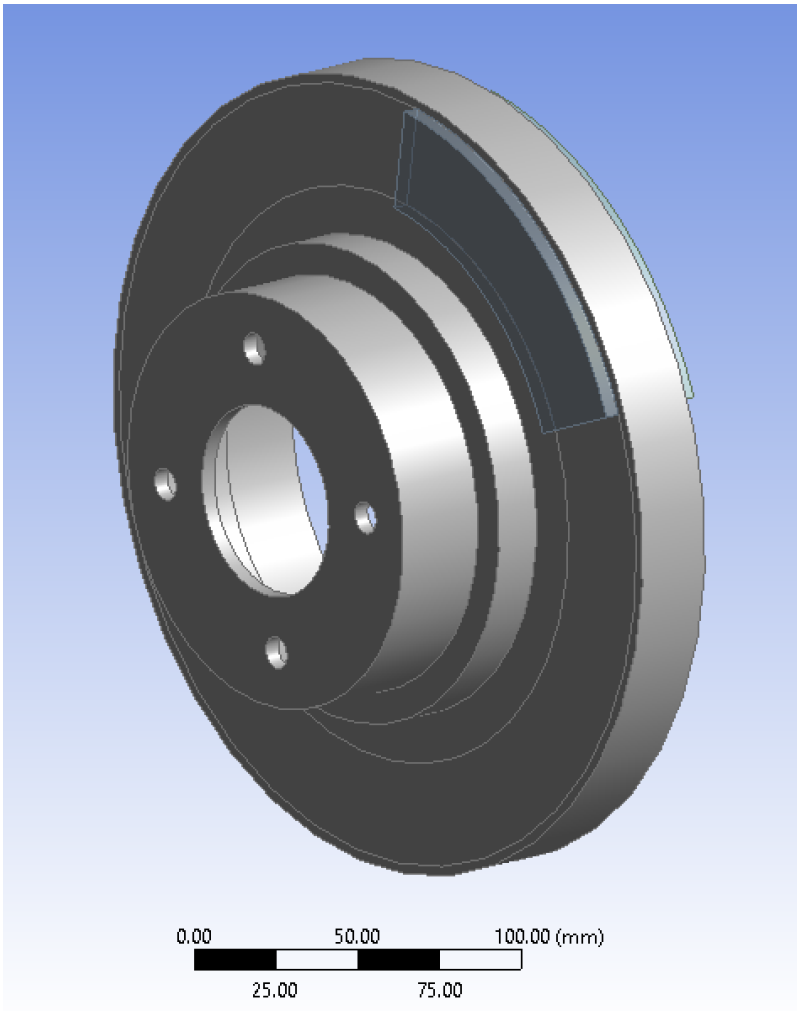

Figure 1. Model of Brake Disc and Brake Pad Geometry

The objective of the brake design problem is to design a minimum-volume brake disc for emergency situations while minimizing the maximum stress, maximizing the first natural frequency, and minimizing maximum temperature of the brake disc.

Model Setup and Analysis

Structural Analysis

Simulation of structural analysis will determine the maximum stress experienced within the material of the brake disc. The brake disc must withstand pressure from the brake pads in emergency braking conditions since the disc experiences induced stresses from friction with the brake pads as well as stresses from centrifugal body forces, so it is essential to minimize the stresses occurring within the disc.

The two materials used for the geometry are structural steel for the pads and gray cast iron for the disc. The geometry was meshed with tetrahedrons with a 3mm element size. Rotational velocity was 250 rad/s in the y-axis of the disc. A revolute joint with a body-ground connection type was added to the innermost part of the disc. A pressure of 10.495 MPa was applied to each brake pad face that frictionally contacts the disc. The x- and z-axis displacement was 0 meters for all faces of the brake pads. Then, the equivalent von-Mises stress solution was obtained with the maximum value indicated as an output parameter. The details and resulting model of the equivalent stress for the brake pads and the brake disc are pictured in Figure 2 and Figure 3 respectively.

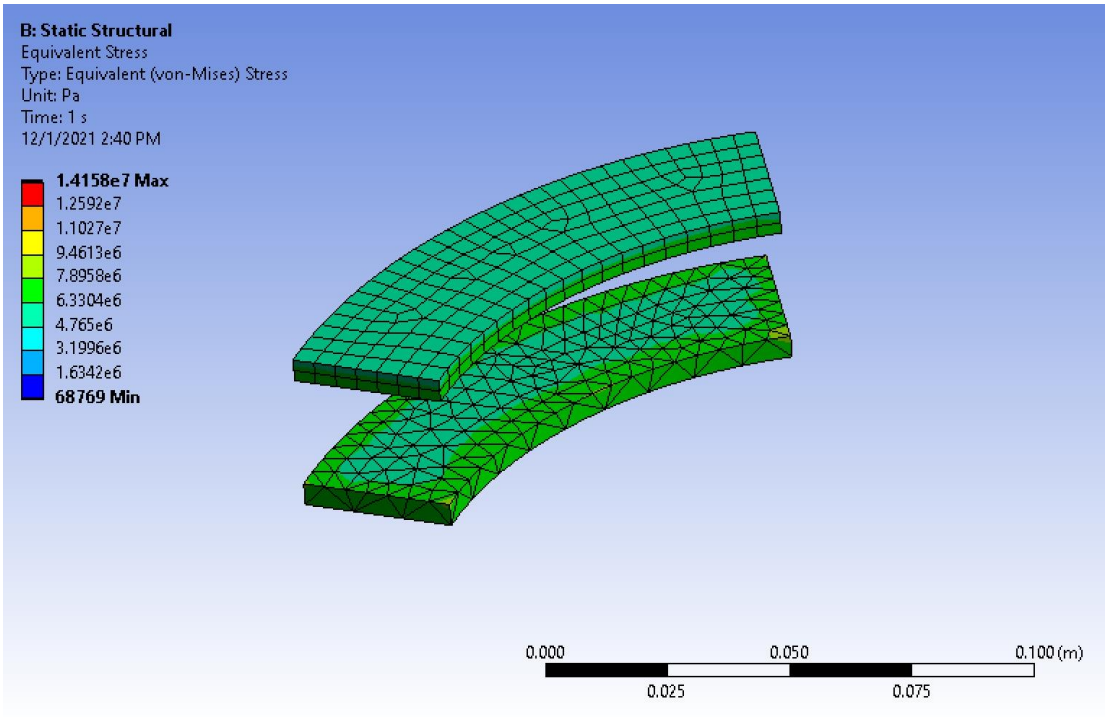

Figure 2. Results of Equivalent von-Mises Stress for Brake Pads

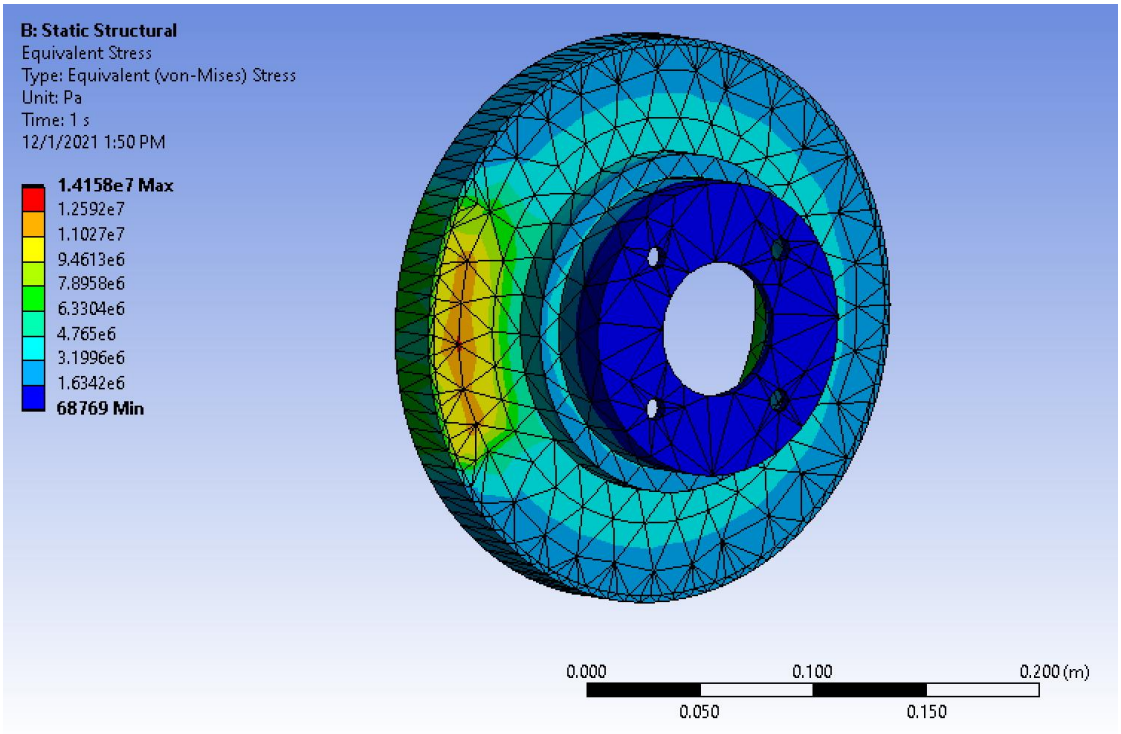

Figure 3. Results of Equivalent von-Mises Stress for Brake Disc

Modal Analysis

Simulation of modal analysis will determine the first natural frequency of the disc. The first natural frequency must be greater than the engine's firing frequency to ensure that the resonance from the engine will not cause the disc to fail, so the goal is to maximize the first natural frequency of the disc.

The maximum modes to find for the brake disc was set to 10. Then, the total deformation was obtained, and the first 7 modes were calculated with the resultant frequency indicated as an output parameter. The details of the frequency results are pictured in Figure 4 with the first natural frequency found in Mode 7. The resulting model with total deformation applied can be seen in Figure 5.

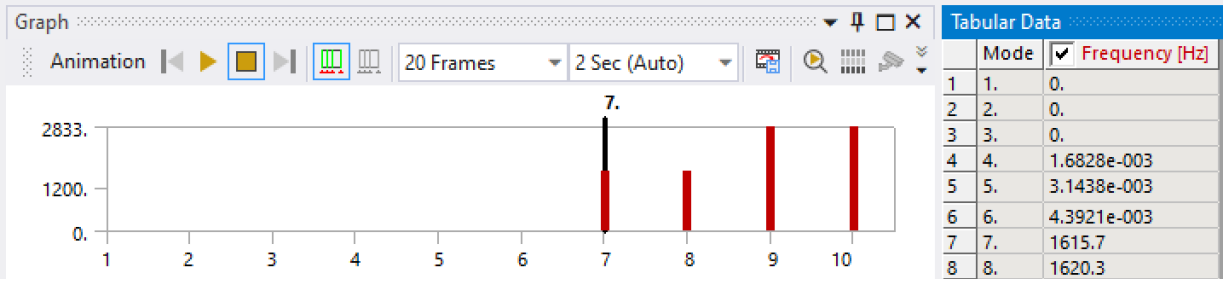

Figure 4. Details of First Natural Frequency – Mode 7

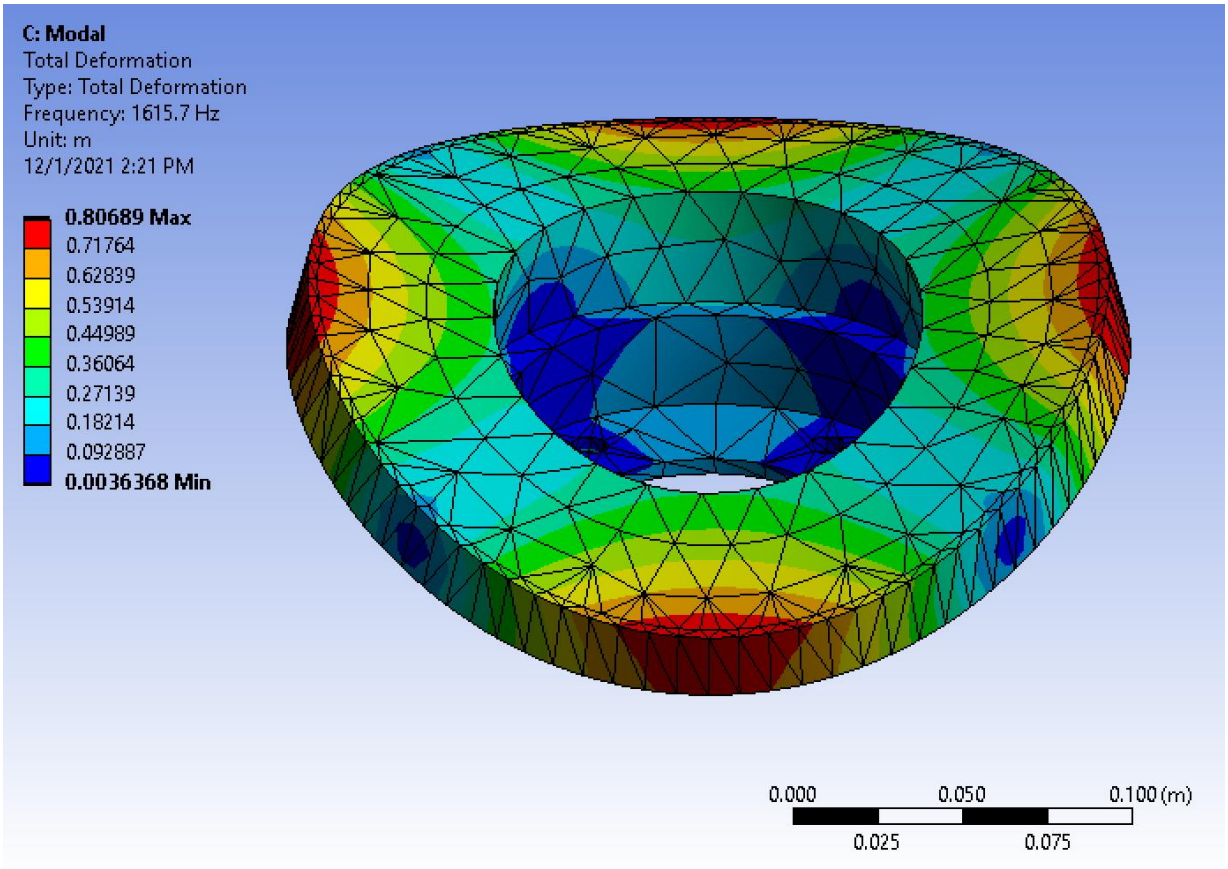

Figure 5. Results of Deformation and Frequency for Brake Disc

Thermal Analysis

Simulation of thermal analysis will determine the maximum temperature of the disc. The brake pads will create friction on the rotor disc which will generate heat flux. This causes the disc to experience an increase in temperature and thermal stresses that can lead to wear and tear of the disc, so it is important to minimize temperatures due to friction.

The initial temperature was set to 35 degrees Celsius. The analysis settings were set such that the number of steps and current step number are each 5. Step end time was 5 seconds. Initial time step was 0.01 seconds, minimum time step was 0.001 seconds, and maximum time step was 0.1 seconds. Convection was set with a film coefficient of 5 W/m^2C and ambient temperature of 35 degrees Celsius. Heat flux with a magnitude of 1.5395 MW/m^2 was applied to each surface that contacts a brake pad. Then, the temperature is obtained with the maximum value indicated as an output parameter. The details and resulting model of the temperature are pictured in Figure 6.

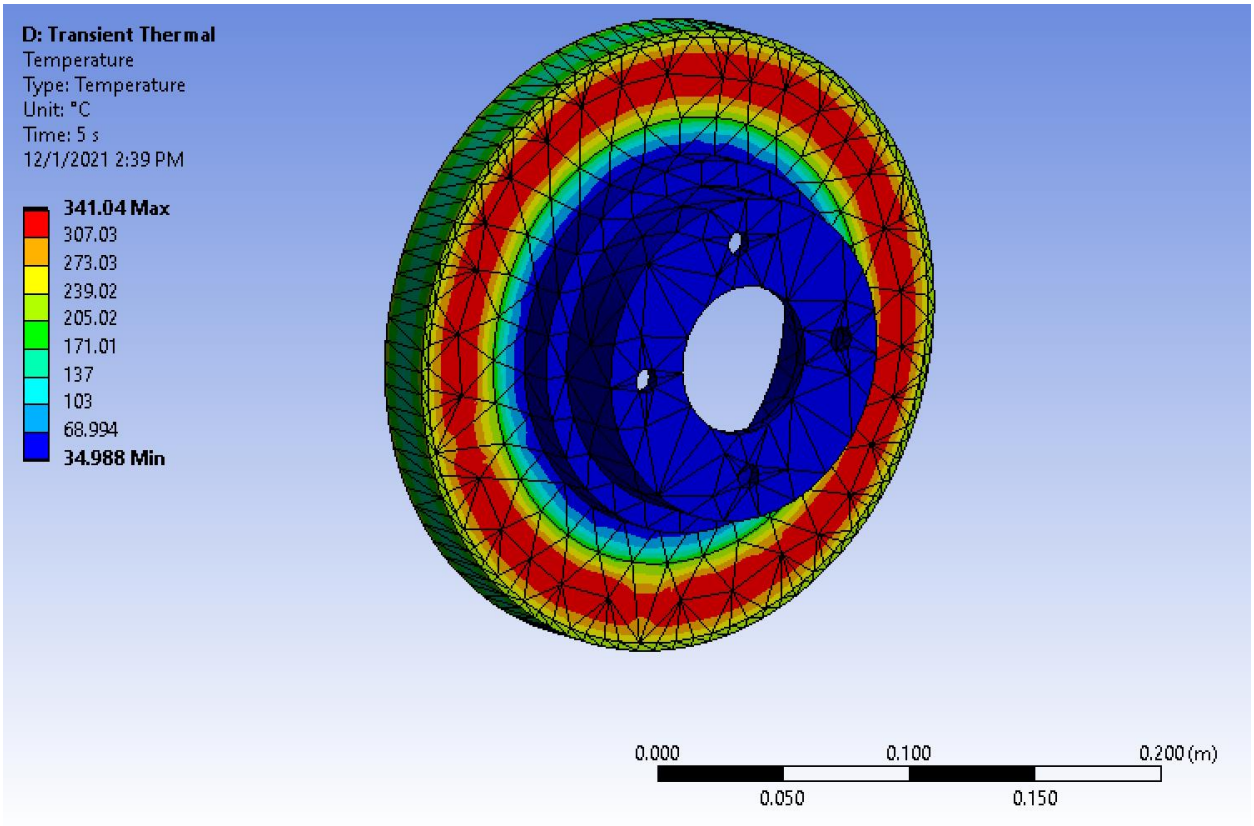

Figure 6. Details and Resulting Model of Temperature

DOE and Optimization

Optimization will help minimize or maximize the objective through an iterative process. A specific DOE methodology will help determine which design to evaluate from design spaces of varying sizes. From this, a statistical prediction can be created for the objective values of other designs with lower uncertainties, and the sensitivity of variables can be determined.

Design Objectives and Constraints

There are four objectives that can potentially be optimized: the maximum equivalent stress, the maximum temperature, the natural frequency, and the disc volume. A Multi-Objective Genetic Algorithm (MOGA) can be utilized to optimize all four objectives simultaneously. An alternative approach is to choose a single objective to optimize while setting all other objectives as constraints. The result is a sequence of solutions called the Pareto Optimal, and a surface that fits through these solutions called the Pareto Frontier which can assist in quantitatively revealing the trade-offs between different objectives.

In this report, the single-objective optimization will be performed using the Nonlinear Programming by Quadratic Lagrangian algorithm in ANSYS. The algorithm is compatible with the current continuous-variable optimization problem; it can quickly identify a local solution and is used when there is only one objective and less than 10 variables or input parameters.

Define Input Parameters

The input parameters are defined in Figure 7 for the model dimensions, where H28 is the rotor thickness, V29 is the rotor outer diameter, and V30 is the rotor inner diameter.

Dimensions: 11	
H18	5 mm
H20	30 mm
H21	35 mm
H27	5 mm
P H28	25 mm
V13	5 mm
V26	30 mm
P V29	125 mm
P V30	75 mm
V31	30 mm
V9	5 mm

Figure 7. Defined Input Parameters

For the response surface, the DOE method chosen was the Latin Hypercube Sampling (LHS) design with 15 samples. The number of samples was later increased to 25 to improve the response surface's fit to the data. The DOE sample ranges for computing the three parameterized inputs are displayed in Table 1. The results of the DOE computations, determined by the input parameter bounds, are displayed in Figure 8.

Table 1. DOE Sample Value Ranges to Compute

	Rotor Thickness	*Rotor Outer Diameter*	*Rotor Inner Diameter*
Lower Bound	20 mm	124 mm	70 mm
Upper Bound	30 mm	160 mm	90 mm

Table of Outline A6: Design Points of Design of Experiments

	A	B	C	D	E	F	G	H
1	Name	P1 - rotor_thickness (mm)	P2 - rotor_OD (mm)	P3 - rotor_ID (mm)	P4 - Equivalent Stress Maximum (Pa)	P5 - Total Deformation Reported Frequency (Hz)	P6 - Temperature Maximum (C)	P7 - Solid Volume (m^3)
2	1	25	139.12	71.2	1.3393E+07	1378.2	340.29	0.0013203
3	2	26.6	149.2	83.2	1.4868E+07	1181.5	337.71	0.0015224
4	3	20.2	142	86.4	1.2741E+07	1156.9	361.56	0.0010586
5	4	25.8	157.84	80.8	1.4424E+07	1079.2	342.33	0.001722
6	5	21	130.48	75.2	1.1557E+07	1468.1	356.4	0.00096208
7	6	29.4	146.32	74.4	1.5074E+07	1335.3	332.25	0.0016754
8	7	25.4	150.64	84	1.426E+07	1123.4	339.97	0.0014914
9	8	29	133.36	81.6	1.5248E+07	1442.6	338.67	0.0012484
10	9	23	152.08	76	1.2998E+07	1130.8	348.66	0.0014686
11	10	22.2	131.92	89.6	2.6719E+07	1209.7	352.33	0.0009189
12	11	23.8	127.6	70.4	1.3279E+07	1613.6	344.33	0.0010425
13	12	21.8	156.4	79.2	1.3266E+07	1038	354.87	0.0014717
14	13	24.6	154.96	76.8	1.375E+07	1110.5	341.89	0.0016175
15	14	27	137.68	87.2	1.5069E+07	1269	337.7	0.0012187
16	15	23.4	159.28	73.6	1.3492E+07	1032.2	347.19	0.0016733
17	16	28.2	136.24	84.8	1.5143E+07	1342.4	336.64	0.001254
18	17	27.8	134.8	78.4	1.4304E+07	1458.9	338.92	0.0012734
19	18	26.2	143.44	88	1.5613E+07	1187.1	338.86	0.001315
20	19	21.4	126.16	77.6	1.1892E+07	1501.8	352.89	0.00088558
21	20	20.6	147.76	88.8	2.7341E+07	1059.9	360.52	0.0011646
22	21	24.2	144.88	82.4	1.3207E+07	1216.3	343.58	0.0013173
23	22	28.6	153.52	72	1.5293E+07	1205.6	333.67	0.0018529
24	23	29.8	140.56	85.6	1.6173E+07	1305.6	332.49	0.0014133
25	24	22.6	129.04	72.8	1.2228E+07	1550.8	349.5	0.0010097
26	25	27.4	124.72	80	1.4076E+07	1552.4	333.5	0.001017

Figure 8. Results of DOE Computations

Response Surface

The response surface method type used was Genetic Aggregation. This method utilizes a genetic algorithm to generate a selection of different responses solved in parallel. After an initial response surface was created, goodness of fit was checked (see Figure 9). Since goodness of fit was sufficient, verification points were then assessed. Six verification points were selected, but goodness of fit was not satisfactory (see Figure 10). Verification point outliers were assigned to be refinement points, and additional verification points were added iteratively. After reaching 18

verification points and 12 refinement points, the number of verification points and refinement points was deemed adequate. Since the goal is to perform optimization, an accurate response surface is not necessary, so working to get a relatively accurate surface model will be sufficient for optimization. Figure 11 displays the final Goodness of Fit plot after all refinement. The numerical results after all iterations, which suggest that the verification points were still performing relatively, can be seen in Figure 12. The resultant point is included in Figure 13. The refinement points and verification points are listed in Figure 14 and Figure 15 respectively.

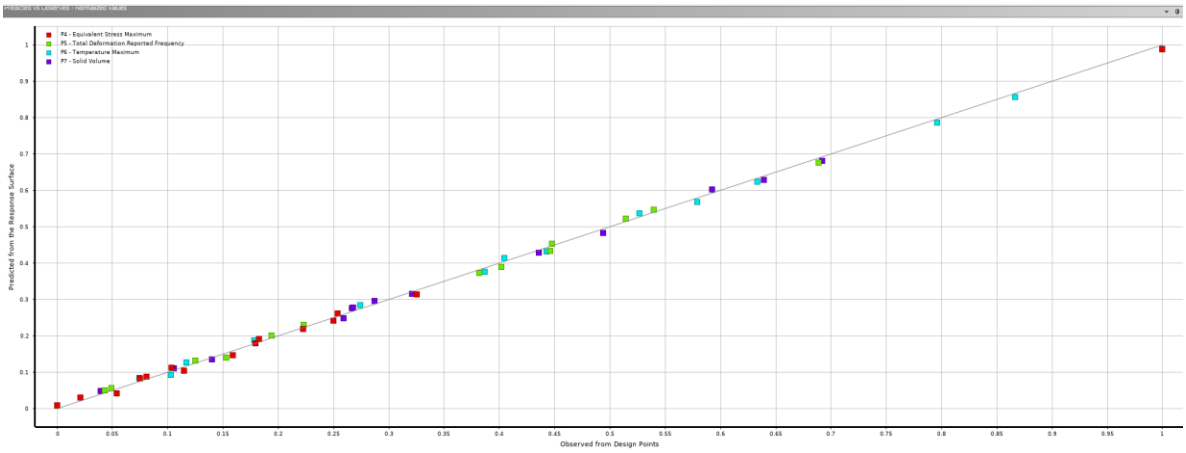

Figure 9. Initial Response Goodness of Fit

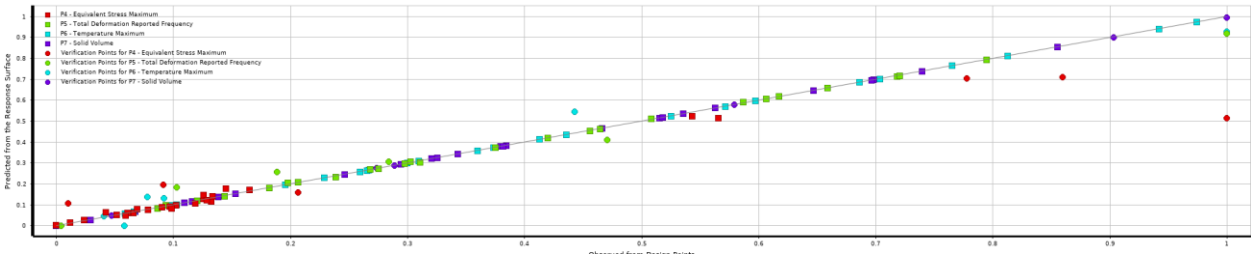

Figure 10. Goodness of Fit for First Iteration of Verification Points

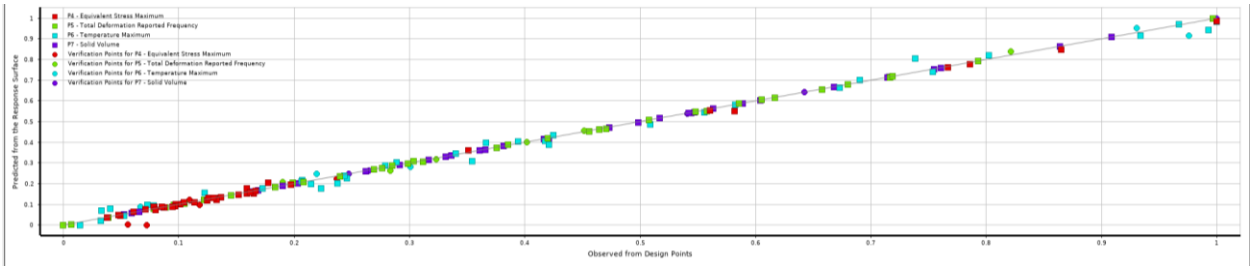

Figure 11. Goodness of Fit for Last Iteration of Verification Points

Table of Schematic E3: Response Surface

	A	B	C	D	E
1		P4 - Equivalent Stress Maximum	P5 - Total Deformation Reported Frequency	P6 - Temperature Maximum	P7 - Solid Volume
2	Coefficient of Determination (Best Value = 1)				
3	Learning Points	0.99855	0.99988	0.99282	1
4	Cross-Validation on Learning Points	0.93451	0.99887	0.94863	1
5	Root Mean Square Error (Best Value = 0)				
6	Learning Points	2.7492E+05	2.2133	0.78296	3.7018E-09
7	Verification Points	6.7298E+05	7.0371	1.0256	3.575E-08
8	Cross-Validation on Learning Points	1.8507E+06	6.7935	2.0936	1.3244E-07
9	Relative Maximum Absolute Error (Best Value = 0%)				
10	Learning Points	11.351	2.5668	22.706	0
11	Verification Points	26.242	7.6033	21.42	0.04508
12	Cross-Validation on Learning Points	64.331	8.081	69.501	0.18638
13	Relative Average Absolute Error (Best Value = 0%)				
14	Learning Points	2.6793	0.81991	6.6609	0
15	Verification Points	5.4344	2.1544	8.6889	0
16	Cross-Validation on Learning Points	19.077	2.7976	16.99	0.027466

Figure 12. Goodness of Fit Results of Response Surface

Table of Outline A24: Response Points

	A	B	C	D	E	F	G	H
1	Name	P1 - rotor_thickness (mm)	P2 - rotor_OD (mm)	P3 - rotor_ID (mm)	P4 - Equivalent Stress Maximum (Pa)	P5 - Total Deformation Reported Frequency (Hz)	P6 - Temperature Maximum (C)	P7 - Solid Volume (m^3)
2	Response Point	25	142	80	1.2191E+07	1288	341.87	0.00131
*	New Response Point							

Figure 13. Response Point

Table of Outline A19: Refinement Points

	A	B	C	D	E	F	G	H
1	Name	P1 - rotor_thickness (mm)	P2 - rotor_OD (mm)	P3 - rotor_ID (mm)	P4 - Equivalent Stress Maximum (Pa)	P5 - Total Deformation Reported Frequency (Hz)	P6 - Temperature Maximum (C)	P7 - Solid Volume (m^3)
2	1	29.925	159.81	89.907	3.9467E+07	1045.7	332.86	0.0019073
3	2	29.898	124.87	70.386	1.4111E+07	1781.8	332.23	0.001195
4	3	23.412	159.37	89.802	3.5561E+07	964.52	344.55	0.0015407
5	4	23.956	125.09	83.671	1.2941E+07	1411.6	344.42	0.0008931
6	5	29.024	124.26	89.74	3.3266E+07	1347.4	331.67	0.00093922
7	6	20.094	158.92	85.303	1.2732E+07	958.91	362.59	0.0013835
8	7	20.302	157.62	70.001	1.2514E+07	991.33	354.39	0.0014664
9	8	24.264	134.22	78.23	1.2768E+07	1419.8	342.71	0.0011293
10	9	28.689	136.68	70.065	1.4228E+07	1520.6	338.23	0.0014359
11	10	25.384	125.52	89.983	3.2701E+07	1277.4	335.05	0.00087738
12	11	26.812	158.73	87.924	2.0646E+07	1023.8	337.96	0.0017295
13	12	20.221	144.81	70.499	1.1837E+07	1194.4	362.38	0.0012124

Figure 14. Refinement Points

Table of Outline A22: Verification Points

	A	B	C	D	E	F	G	H
1	Name	P1 - rotor_thickness (mm)	P2 - rotor_OD (mm)	P3 - rotor_ID (mm)	P4 - Equivalent Stress Maximum (Pa)	P5 - Total Deformation Reported Frequency (Hz)	P6 - Temperature Maximum (C)	P7 - Solid Volume (m^3)
2	1	29.925	159.81	89.907	3.9467E+07	1045.7	332.86	0.0019073
3	2	29.898	124.87	70.386	1.4111E+07	1781.8	332.23	0.001195
4	3	20.221	144.81	70.499	1.1837E+07	1194.4	362.38	0.0012124
5	4	23.412	159.37	89.802	3.5561E+07	964.52	344.55	0.0015407
6	5	29.024	124.26	89.74	3.3266E+07	1347.4	331.67	0.00093922
7	6	29.939	159.74	80.921	1.7328E+07	1115.8	333.31	0.0020165
8	7	23.956	125.09	83.671	1.2941E+07	1411.6	344.42	0.0008931
9	8	20.443	142.68	78.876	1.2072E+07	1225.9	360.42	0.0011328
10	9	20.07	127.08	84.454	1.2559E+07	1332	361.83	0.00081387
11	10	20.302	157.62	70.001	1.2514E+07	991.33	354.39	0.0014664
12	11	20.094	158.92	85.303	1.2732E+07	958.91	362.59	0.0013835
13	12	28.689	136.68	70.065	1.4228E+07	1520.6	338.23	0.0014359
14	13	24.264	134.22	78.23	1.2768E+07	1419.8	342.71	0.0011293
15	14	25.384	125.52	89.983	3.2701E+07	1277.4	335.05	0.00087738
16	15	26.901	126.9	73.362	1.3647E+07	1637	336.39	0.0011117
17	16	26.812	158.73	87.924	2.0646E+07	1023.8	337.96	0.0017295
18	17	24.865	150.78	70.114	1.3632E+07	1192.9	340.65	0.0015867
19	18	26.184	144.87	76.133	1.3884E+07	1290.7	338.11	0.0014647

Figure 15. Verification Points

The response curves for each of the parameters are displayed below. It can be seen in Figure 16, Figure 17, Figure 18, Figure 20, and Figure 23 that monotonicity can be observed within the constraints of the design points for this simulation. As rotor thickness increases, equivalent stress also increases (Figure 16) due to moments and required forces needed to halt the rotor. As rotor thickness increases, natural frequency increases (Figure 17) which is likely due to the greater amount of material able to withstand vibrations. As rotor thickness increases, temperature decreases (Figure 18) which may be due to greater heat flux distribution throughout the body of the rotor. As the outer diameter of the rotor increases, natural frequency decreases (Figure 20) which is likely due to larger moments and larger surface areas for contact and vibration. As the inner diameter of the rotor increases, the natural frequency decreases (Figure 23) which may be due to larger moments of inertia allowing for vibrations. As for trends for the Solid Volume, one example can be seen in Figure 25 where an increase in rotor outer diameter will allow for the solid volume to increase. Similarly, if the thickness of the rotor increases, volume will increase, and if

the inner diameter of the rotor increases, material is being removed from the body and the volume will decrease.

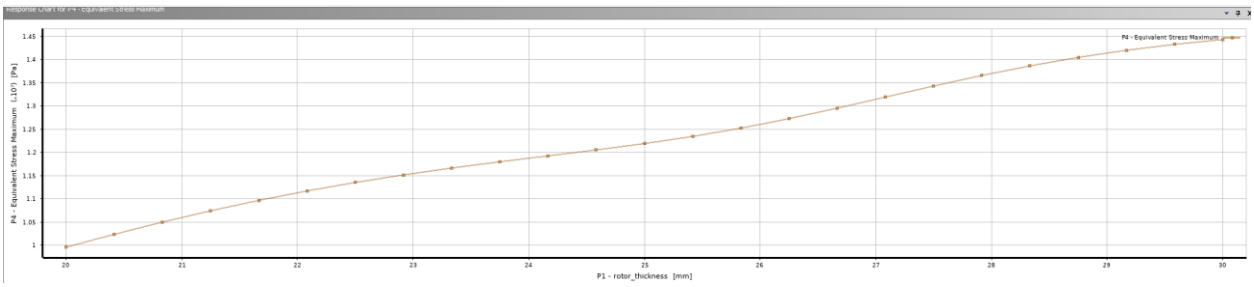

Figure 16. Response Curve for Rotor Thickness and Equivalent Stress

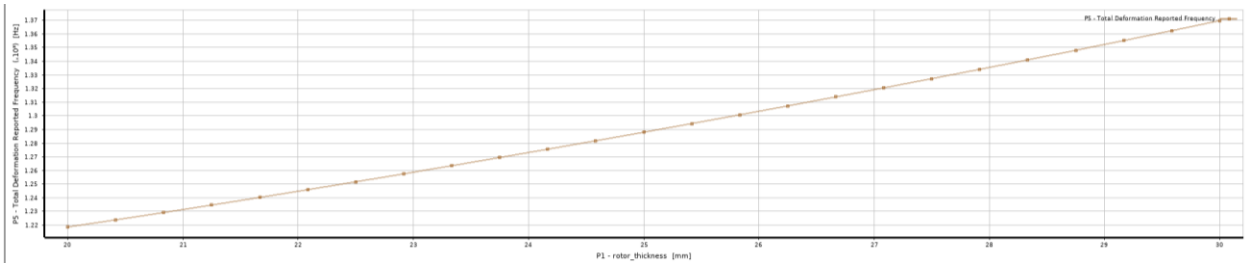

Figure 17. Response Curve for Rotor Thickness and Frequency

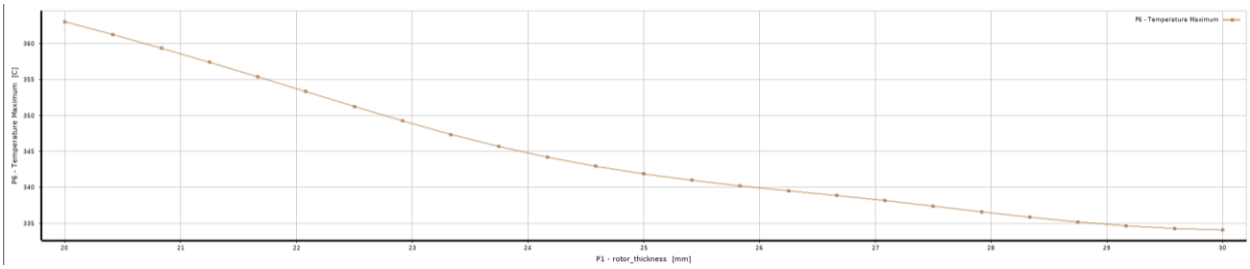

Figure 18. Response Curve for Rotor Thickness and Temperature

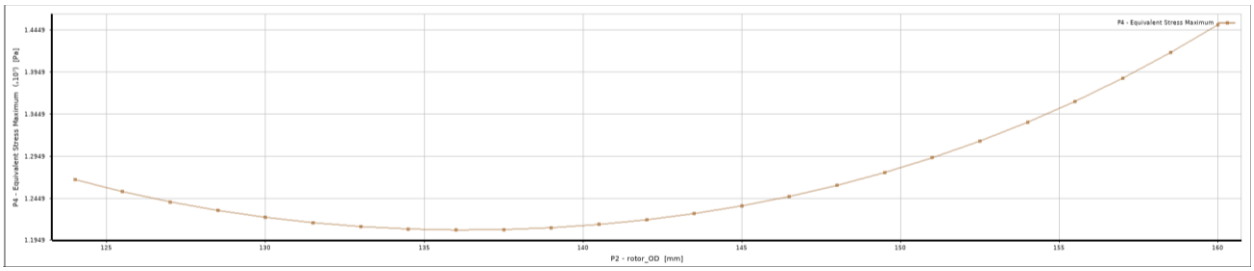

Figure 19. Response Curve for Rotor Outer Diameter and Equivalent Stress

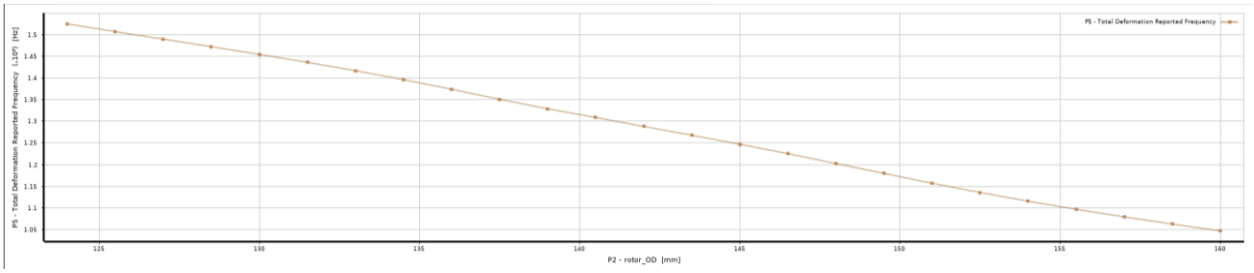

Figure 20. Response Curve for Rotor Outer Diameter and Frequency

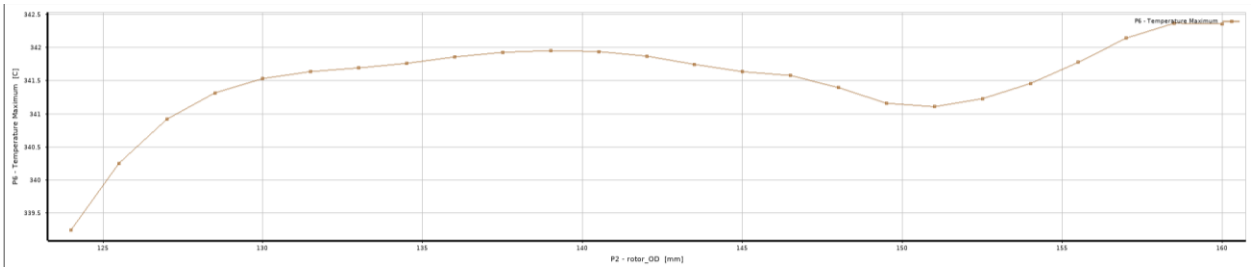

Figure 21. Response Curve for Rotor Outer Diameter and Temperature

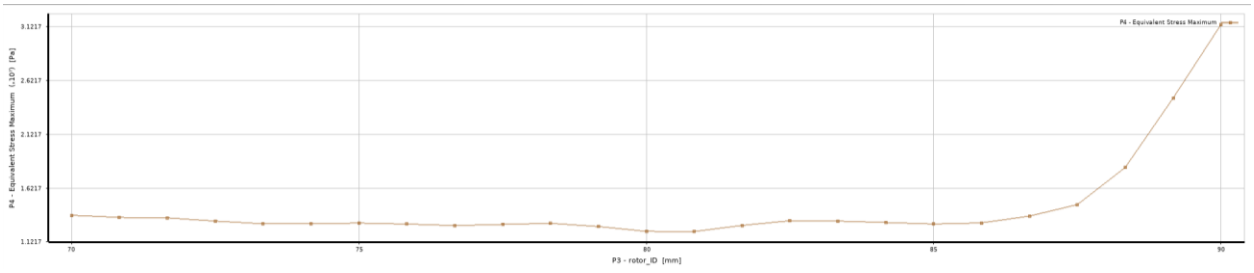

Figure 22. Response Curve for Rotor Inner Diameter and Equivalent Stress

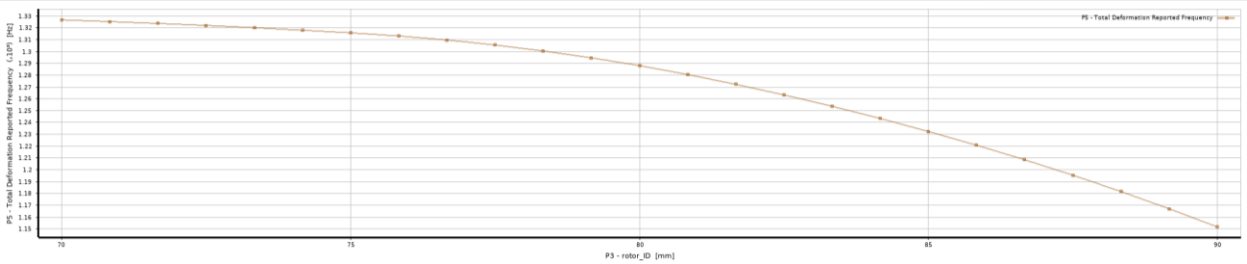

Figure 23. Response Curve for Rotor Inner Diameter and Frequency

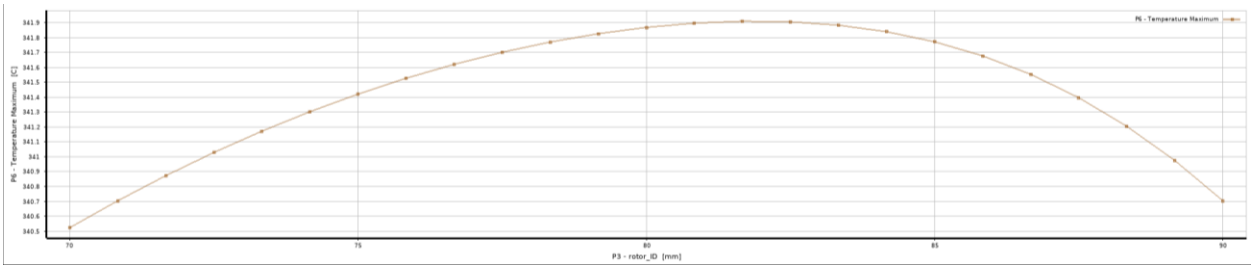

Figure 24. Response Curve for Rotor Inner Diameter and Temperature

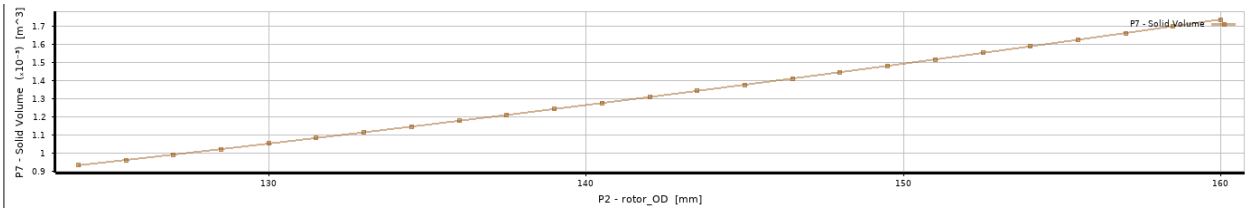

Figure 25. Response Curve for Rotor Outer Diameter and Solid Volume

Sensitivity Analysis

Below, in Figure 26, the local sensitivity is graphed. This plot shows the norm of each partial derivative with respect to the selected variables. Based on the results of the simulation, certain input parameters will have significant influence on the output parameters:

- Increasing rotor inner diameter will cause the equivalent stress to increase
- Increasing rotor outer diameter will cause the natural frequency to decrease
- Increasing rotor thickness will cause temperatures to decrease
- Increasing rotor outer diameter will have the greatest impact on increasing solid volume

Certain variables affect the optimization more than others. Rotor thickness has a huge impact on the temperature analysis and rotor inner diameter has an important influence on the equivalent stress maximum. In terms of optimizing the volume, which is the main objective of this project, rotor thickness and rotor outer diameter are important in the final resultant volume of the brake disc.

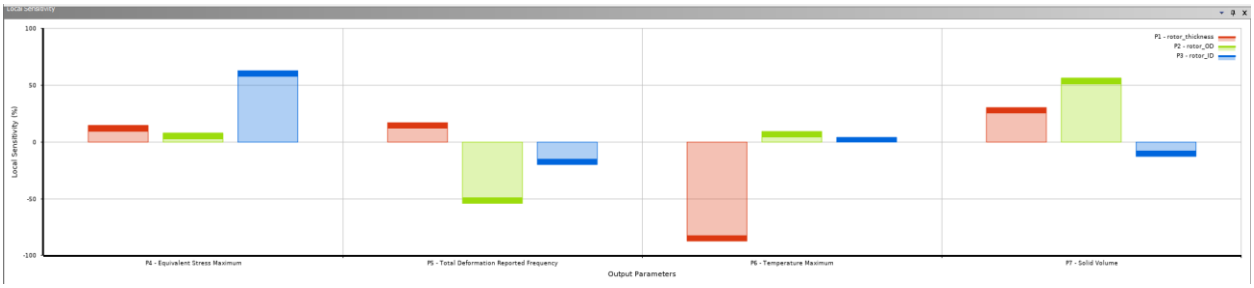

Figure 26. Local Sensitivity

The local sensitivity curves summarize the response curves into categorical plots based on the output variable selected (see Figure 27, Figure 28, and Figure 29). Monotonicity can be easily observed in curves related to equivalent stress and natural frequency. The sensitivity curves tend to increase for maximum equivalent stress and tend to decrease for natural frequency (except for rotor thickness that causes natural frequency to increase when the thickness increases).

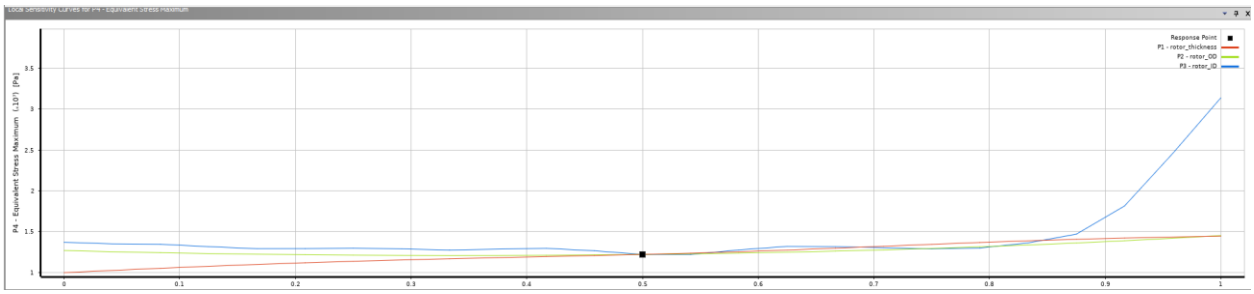

Figure 27. Local Sensitivity Curves for Equivalent Stress

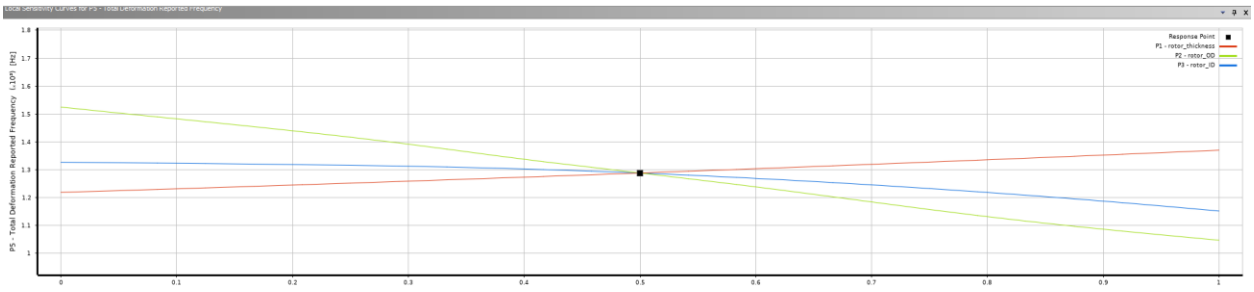

Figure 28. Local Sensitivity Curves for Frequency

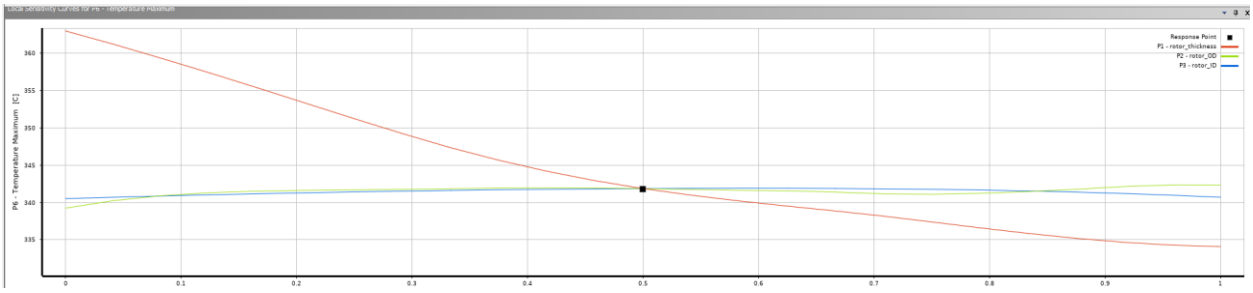

Figure 29. Local Sensitivity Curves for Temperature

Optimization

The design variables are the rotor thickness, the rotor outer diameter, and the rotor inner diameter. The constraints for this single-objective problem are defined as follows:

Maximum equivalent stress ≤ 17 MPa

Natural frequency ≥ 1100 Hz

Temperature ≤ 400˚C

The objective of this problem is to minimize the volume of the brake disc. The potential trade-offs include:

- Increasing rotor outer diameter that cause the natural frequency to decrease
- Increasing rotor thickness which will increase the solid volume
- Increasing rotor thickness that help decrease temperature, but it will increase solid volume

See Figure 30 for optimization curves and constraints used.

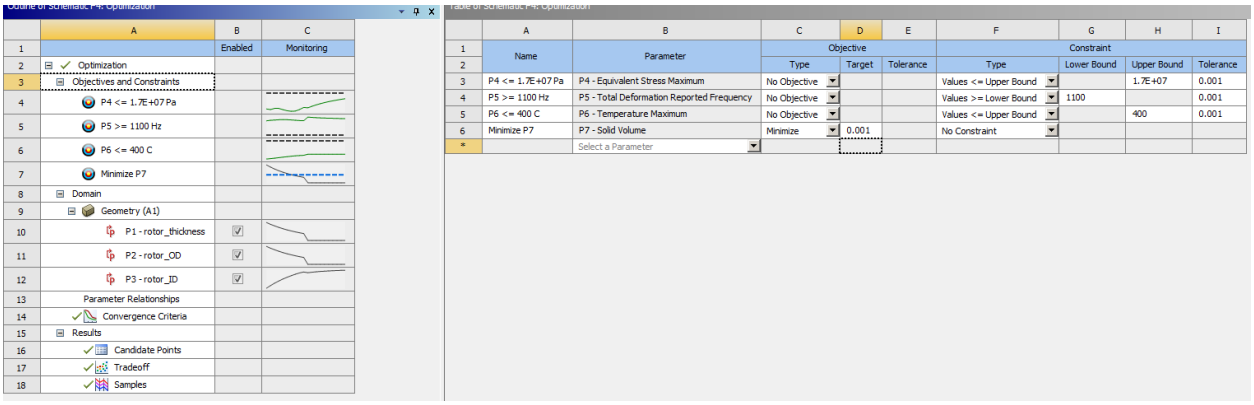

	A	B	C
1		Enabled	Monitoring
2	Optimization		
3	Objectives and Constraints		
4	P4 <= 1.7E+07 Pa		
5	P5 >= 1100 Hz		
6	P6 <= 400 C		
7	Minimize P7		
8	Domain		
9	Geometry (A1)		
10	P1 - rotor_thickness	☑	
11	P2 - rotor_OD	☑	
12	P3 - rotor_ID	☑	
13	Parameter Relationships		
14	Convergence Criteria		
15	Results		
16	Candidate Points		
17	Tradeoff		
18	Samples		

	A	B	C	D	E	F	G	H	I
1	Name	Parameter	Objective			Constraint			
2			Type	Target	Tolerance	Type	Lower Bound	Upper Bound	Tolerance
3	P4 <= 1.7E+07 Pa	P4 - Equivalent Stress Maximum	No Objective			Values <= Upper Bound		1.7E+07	0.001
4	P5 >= 1100 Hz	P5 - Total Deformation Reported Frequency	No Objective			Values >= Lower Bound	1100		0.001
5	P6 <= 400 C	P6 - Temperature Maximum	No Objective			Values <= Upper Bound		400	0.001
6	Minimize P7	P7 - Solid Volume	Minimize	0.001		No Constraint			
*		Select a Parameter							

Figure 30. Optimization Curves

The candidate points are shown in Figure 31. Candidate 1 (verified) was selected as the optimal solution due to its significant reduction in volume while remaining within the designed constraints of the problem. The volume reduction was 24.97%. The equivalent stress maximum was reduced by 8.61%, natural frequency was reduced by 20.44%, and temperature increased by 7.04% from the original design. Despite some slight adjustments that may not have been ideal (increase in temperature and decrease in natural frequency), the candidate point remained within constraints and successfully reduced volume of the brake disc.

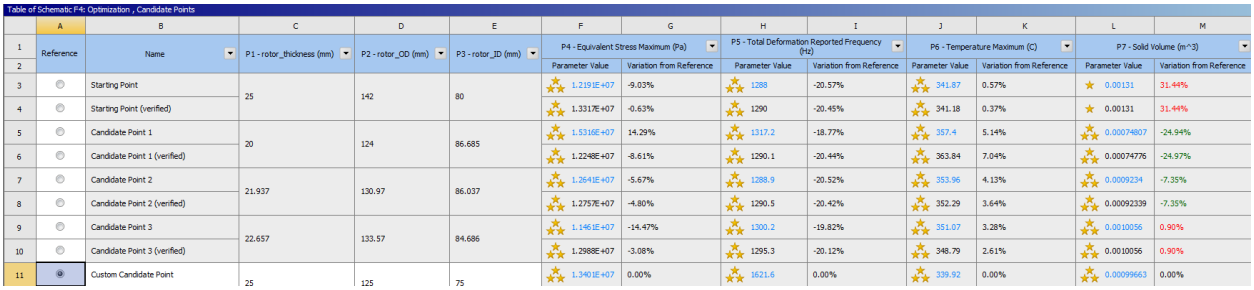

Table of Schematic P4: Optimization , Candidate Points

	A	B	C	D	E	F	G	H	I	J	K	L	M
1	Reference	Name	P1 - rotor_thickness (mm)	P2 - rotor_OD (mm)	P3 - rotor_ID (mm)	P4 - Equivalent Stress Maximum (Pa)		P5 - Total Deformation Reported Frequency (Hz)		P6 - Temperature Maximum (C)		P7 - Solid Volume (m^3)	
2						Parameter Value	Variation from Reference	Parameter Value	Variation from Reference	Parameter Value	Variation from Reference	Parameter Value	Variation from Reference
3	○	Starting Point	25	142	80	1.2191E+07	-9.03%	1288	-20.57%	341.87	0.57%	0.00131	31.44%
4	○	Starting Point (verified)				1.3317E+07	-0.63%	1290	-20.45%	341.18	0.37%	0.00131	31.44%
5	○	Candidate Point 1	20	124	86.685	1.5316E+07	14.29%	1317.2	-18.77%	357.4	5.14%	0.0074807	-24.94%
6	○	Candidate Point 1 (verified)				1.2248E+07	-8.61%	1290.1	-20.44%	363.84	7.04%	0.0074776	-24.97%
7	○	Candidate Point 2	21.937	130.97	86.037	1.2641E+07	-5.67%	1288.9	-20.52%	353.96	4.13%	0.0009234	-7.35%
8	○	Candidate Point 2 (verified)				1.2757E+07	-4.80%	1290.5	-20.42%	352.29	3.64%	0.00092339	-7.35%
9	○	Candidate Point 3	22.657	133.57	84.686	1.1461E+07	-14.47%	1300.2	-19.82%	351.07	3.28%	0.0010056	0.90%
10	○	Candidate Point 3 (verified)				1.2988E+07	-3.08%	1295.3	-20.12%	348.79	2.61%	0.0010056	0.90%
11	◉	Custom Candidate Point	25	125	75	1.3401E+07	0.00%	1621.6	0.00%	339.92	0.00%	0.0009663	0.00%

Figure 31. Candidate Points

See Figure 32 for a comparison of the optimal design against the initial one. The optimal design is reasonable considering the dimensions of each part of the rotor and given the expected results based on initial analysis in ANSYS. The optimal candidate had a lower rotor thickness, a lower rotor outer diameter, and a higher rotor inner diameter. According to the local sensitivity plot (Figure 26), higher rotor inner diameter would cause maximum equivalent stress to increase, which was proven in this simulation. Additionally, when thickness decreases, temperature is

expected to increase, as demonstrated by these results. Lastly, reductions in the rotor outer diameter is expected to reduce the volume of the disc, which helped achieve the objective.

Original Design:

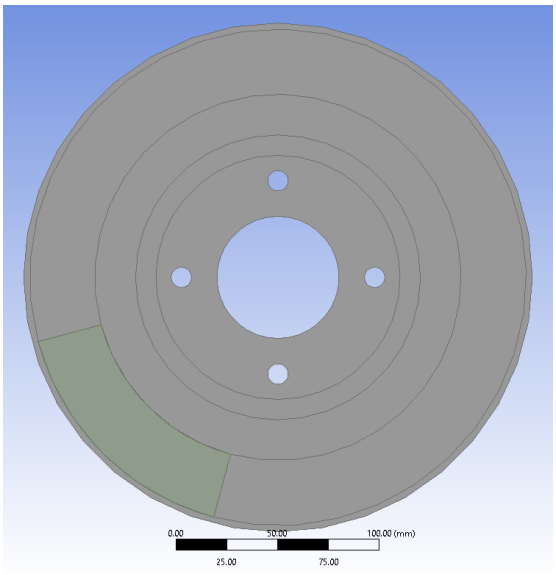

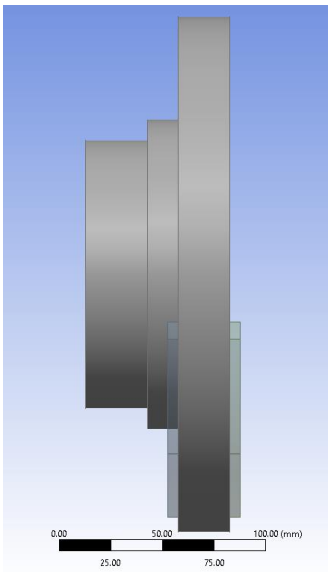

Optimized Design

(24.97% Reduction of Volume):

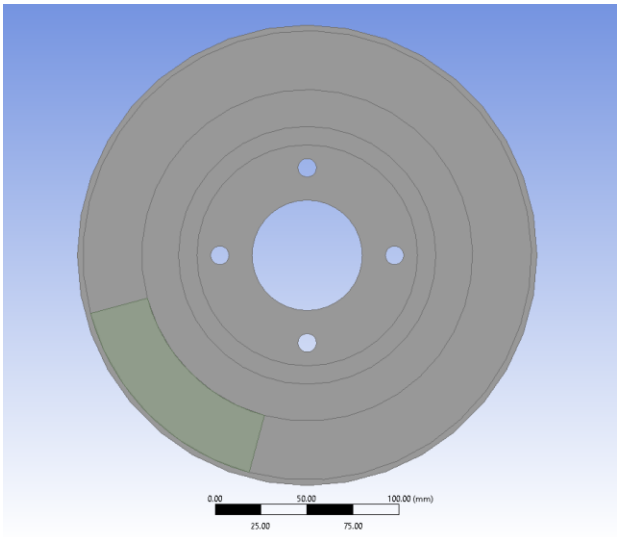

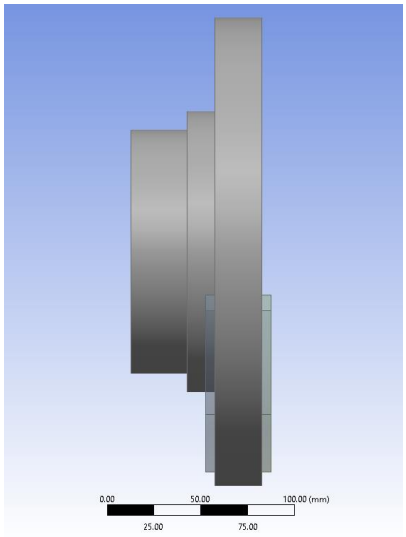

Figure 32. Comparison of Optimal Design vs the Initial One